Physics Letters B 807 (2020) 135574

Contents lists available at ScienceDirect

Physics Letters B

www.elsevier.com/locate/physletb

Antimatter as macroscopic dark matter

Jagjit Singh Sidhu [a,*], Robert J. Scherrer [b], Glenn Starkman [a]

[a] Physics Department/CERCA/ISO Case Western Reserve University, Cleveland, OH 44106-7079, USA
[b] Department of Physics & Astronomy, Vanderbilt University, Nashville, TN 37235, USA

ARTICLE INFO

Article history:
Received 1 June 2020
Received in revised form 16 June 2020
Accepted 18 June 2020
Available online 30 June 2020
Editor: M. Trodden

ABSTRACT

Antimatter macroscopic dark matter (macros) refers to a generic class of antimatter dark matter candidates that interact with ordinary matter primarily through annihilation with large cross-sections. A combination of terrestrial, astrophysical, and cosmological observations constrain a portion of the anti-macro parameter space. However, a large region of the parameter space remains unconstrained, most notably for nuclear-dense objects.

1. Introduction

The evidence for dark matter is overwhelming (see, e.g., [1] and references therein), but the nature of dark matter remains one of the great unsolved mysteries of modern cosmology. While the most well-studied candidates are particle candidates such as WIMPs and axions, it remains an open possibility that dark matter is comprised entirely of macroscopic bound states of fundamental particles. An intriguing possibility is that the such objects could be made of Standard Model quarks or baryons bound by Standard Model forces. This suggestion was originally made by Witten [2], in the context of a first-order QCD phase transition early in the history of the Universe. Others have suggested non-Standard Model versions of such nuclear objects and their formation, for example incorporating the axion [3–10]. The Axion Quark Nugget (AQN) model is the most well-studied model of antimatter macroscopic dark matter in the literature. These nuggets can be made of matter as well as antimatter during the QCD phase transition. A direct consequence of this feature is that the dark matter and baryon densities will automatically assume the same order of magnitude without any fine tuning. This is a consequence of CP violation in the system [5,6], which results in the formation of a different number of nuggets and anti-nuggets This difference is always an order one effect irrespective of the parameters of the theory. However, the nuggets in the AQN model possess a high reflectivity owing to the large potential of the confining layer of axions [4]. In this manuscript, we consider a more generic class of anti-macros in which the anti-macro is not bound by some external layer but by a force sourced by the anti-macro components themselves. Hence, we will assume negligible reflectivity. However, we remain agnostic about the details of this binding force and consider only the phenomenology of such objects.

In recent years the authors have explored the proposition that the dark matter might be macroscopic, in the sense of having a characteristic mass M_x and cross-sectional area in the gram and cm^2 range, respectively [11–18]. The dark matter constituents in this model are called "macros." The macro model has two undetermined parameters, the macro mass M_x and the interaction cross section σ_x. The dominant interaction is assumed to be elastic scattering, with σ_x taken to be the geometric cross-section of the macro.

We begin by first briefly reviewing the existing constraints on macros derived in previous works. For macro masses $M_x \leq 55\,g$ careful examination of specimens of old mica for tracks made by passing dark matter [11,19,20] has ruled out such objects as the primary dark-matter candidate. For $M_x \geq 10^{23}\,g$, a variety of microlensing searches have constrained the abundance of macros [21–25] from a lack of magnification of sources by a passing macro along the line of sight of the observer.

A large region of parameter space was constrained by considering thermonuclear runaways triggered by macros incident on white dwarfs [26]. However, it was later shown [17] that the excluded region of macro parameter space for macros providing all of the dark matter was too large, and more accurate constraints were placed. Dark matter-photon elastic interactions were used together with the Planck Cosmic Microwave Background (CMB) data to constrain macros of sufficiently high reduced cross-section σ_x/M_x [27]. The region of parameter space where macros would have produced obvious devastating injuries was also constrained [15].

In addition to these constraints, limits from possible future observations have also been proposed. Ultra-high-energy cosmic ray detectors that exploit atmospheric fluorescence could potentially

* Corresponding author.
E-mail addresses: jxs1325@case.edu (J.S. Sidhu), robert.scherrer@vanderbilt.edu (R.J. Scherrer), glenn.starkman@case.edu (G. Starkman).

https://doi.org/10.1016/j.physletb.2020.135574

be modified to probe parts of macro parameter space [13], including macros of nuclear density. This analysis has led to constraints being placed using networks of cameras that were originally built to study bolides, i.e. extremely bright meteorites [16]. Some of us have also suggested how the approach applied to mica [19,20] could be applied to a larger, widely available sample of appropriate rock [14], and used to search for larger-mass macros. In addition to that, we have identified additional regions of parameter space constrained by the duration between back-to-back superbursts (thermonuclear runaway on the outer surface of a neutron star) [17].

It is unlikely that macro masses beyond $\sim 10^9$ g could be probed by any purpose-built terrestrial detector assuming even an observation time of a century and a target area the size of the Earth. Terrestrial probes (e.g. ancient rocks [14,19,20]) could have been continuously exposed for up to $\sim 3 \times 10^9$ years, but we are unlikely to carefully examine the more than 1 km^2 that would be needed to push beyond $M_x \sim 10^9$ g. It will therefore require innovative thinking about astrophysical probes (e.g. [26]) to probe the remaining parameter space at the very highest masses.

In this paper, we consider a related but phenomenologically very different macro model: the possibility that macros are composed of antimatter. We dub these objects "anti-macros". While some macro limits simply carry over to the anti-macro case, we will show that this model yields a rich variety of new phenomena, and we will derive corresponding limits on the anti-macro parameter space.

Anti-macros corresponding to the models mentioned in the previous paragraph would most likely have densities that are comparable to nuclear density (which we take to be $\rho_{nuclear} \approx 3.6 \times 10^{14}\,\mathrm{g\,cm^{-3}}$). This is much higher than ordinary "atomic density" ($\rho_{atomic} \approx 1\,\mathrm{g\,cm^{-3}}$), but much lower than the density of black holes of masses in the range we consider. Although anti-macros of approximately nuclear density are of particular interest, other densities are not excluded at this point, so we will consider the full range of possibilities for M_X and σ_X.

The sensitivity of a detector to anti-macros depends on the energy transferred when the anti-macro transits the detector. Consider an anti-macro with cross section σ_X passing through a detector. The energy per unit length deposited by a macro through annihilation in the detector is

$$\frac{dE}{dx} = \kappa \sigma_x \rho c^2, \tag{1}$$

where ρ is the density of the target and κ is introduced, generically, to account for the fraction of the annihilation energy that is deposited as heat into the surrounding medium. In the case of the AQN, $\kappa \ll 1$ in most cases of interest, and the energy deposition is highly suppressed. An order of magnitude estimate is typically $\kappa \sim 10^{-12}$ (see Appendix C in reference [9]). For such objects, the energy deposition is similar to the case of ordinary macros [11–18] and the constraints presented in those references apply to both macros and anti-macros. The energy transfer expression for ordinary macros is

$$\frac{dE}{dx} = \sigma_x \rho v_x^2, \tag{2}$$

where $v_x \sim 250\,\mathrm{km\,s^{-1}}$ is the speed of the macro. Thus, anti-macros with $\kappa \sim 1$ are expected to deposit $\sim 10^6$ times more energy in a target than macros of the same cross-section. They should, in general, be easier to observe. The physical reason for this difference is that the anti-macro collisions with ordinary matter convert rest energy into thermal energy, while macro scattering off of ordinary matter is purely elastic.

To estimate the fraction of energy that thermalizes in the anti-macro, we consider $p\bar{p}$ annihilation.[1] This predominantly results in multi-pion states, with 43% of the final states including 2 charged pions and 49% including 4 charged pions [30], for an average charged pion multiplicity of 3, and a neutral pion multiplicity of 2 [31]. The charged pion lifetime is 3×10^{-8} s, while the neutral pion lifetime is 10^{-16} s [1]. Thus, all of the neutral pions decay essentially where they were produced into 2 high energy gamma rays [1], while the charged pions or their decay products are likely to escape the macro. We therefore expect that 4 gamma ray photons carrying ~ 100 MeV are produced per annihilation interaction. Following [10], such photons are expected to thermalize within the anti-macro, resulting in an emission temperature of $T_{surf} = 10^7$ K from the non-degenerate part of the positron atmosphere, with the emission spectrum expected to be strongly peaked at 1 keV energies. Thus, $\kappa \sim 0.4$.

The preceding arguments are relevant to anti-macros that are able to travel through the overburden of a detector and leave a detectable signal within it. The speed of an anti-macro traveling through a medium can be determined from Newton's second law

$$M_x \frac{dv_x}{dt} = \kappa \rho \sigma_x c^2\,. \tag{3}$$

In the absence of any accelerating forces Equation (3) evolves as

$$v^2 = v_{X,0}^2 - 2\kappa \frac{\sigma_x}{M_x} \langle \rho x \rangle c^2\,, \tag{4}$$

where $\langle \rho x \rangle = \int \rho dx$ is the column density encountered by the anti-macro passing through the medium. Anti-macros with too high a value of σ_x/M_x would not have been expected to encounter a detector but rather fall vertically reaching some terminal velocity. Indeed for $\sigma_x/M_x \geq 10^{-12}\,\mathrm{g\,cm^2}$ an anti-macro is not expected to reach far below the surface of the Earth, while for $\sigma_x/M_x \geq 10^{-9}\,\mathrm{g\,cm^2}$, the anti-macro is not expected to penetrate to the bottom of the atmosphere with any of its initial kinetic energy.

The rest of this paper is outlined as follows. In Section 2, we constrain a wide region of parameter space by requiring that the energy deposited by anti-macros in the early Universe not alter the CMB significantly. In Section 3, we perform a similar calculation for big bang nucleosynthesis (BBN), where the main constraint in this case is the requirement that annihilation with helium-4 not overproduce lighter elements. In Section 4, we place constraints for anti-macros that would have caused unexpected deaths in the well-monitored population of the Western world over the past decade. In section 5, we discuss constraints on anti-macros that are of a similar order-of-magnitude to that of regular macros.

2. Cosmic microwave background constraints

WIMPs annihilating and dumping energy into the photon-baryon fluid would drastically alter the CMB, leading to changes in both the temperature and polarization power spectra. As such, CMB anisotropies offer an opportunity to constrain the nature of dark matter. Constraints have been placed on the thermally averaged cross section of WIMPS based on the observed spectrum [28]. We will use this result to constrain anti-macros annihilating with protons in the pre-recombination fluid. The way in which dark matter annihilations heat the fluid depends on the nature of the cascade of particles produced following the annihilations. The

[1] This is a model dependent assumption. For models with different constituents, the relevant branching ratios must be calculated. However, our results remain relevant as long as the main branching ratio(s) that contribute to thermalization of the anti-macro deposit a similar amount, say within a factor of a few, of the energy produced from annihilation.

fraction of the rest mass energy that is injected into the gas can be modelled by an efficiency factor, $f(z)$. Computations for various channels can be found in [29]. For all cases considered in [29], $f(1100) \sim 0.3$ and in some cases it is closer to unity. As discussed earlier, in the case of anti-macros, the fraction of energy that we expect to contribute to the heating of the surrounding medium is $\kappa \sim 0.4$. Thus, we neglect a detailed calculation and take both values to be equal to each other for simplicity.

Anti-macros would consist of a reasonable fraction of anti-protons that would annihilate with incident protons in the pre-recombination fluid. For WIMPS, which were generically considered in placing the bounds in reference [28], the energy density injection rate is

$$\dot{\rho}_\chi = n_\chi^2 \langle \sigma_\chi v \rangle (2 m_B c^2) \,. \tag{5}$$

The analogous quantity for macros is

$$\dot{\rho}_x = n_x n_B \langle \sigma_x v \rangle (2 m_B c^2) \,. \tag{6}$$

By equating the two energy injection expressions and utilizing the bounds from [28], we can determine the constrained region for anti-macros. This bound can be expressed as

$$\frac{\sigma_x}{M_x} < 2 \times 10^{-10} \frac{\mathrm{cm}^2}{\mathrm{g}} \,. \tag{7}$$

Macros above this bound, plotted in grey in Fig. 1, would have deposited too much energy in the early Universe and altered the observed CMB spectra and are thus ruled out as being all the dark matter.

3. Big bang nucleosynthesis constraints

The effects of antimatter injection on BBN have long been a topic of study [32–38]. For the particular case of the AQN model, one obtains a suppression of heavy elements including lithium as a generic feature irrespective of any specifics of the model [8]. This effect occurs due to the capture and subsequent annihilation of Li and Be ions by the AQN. These heavier ions interact more strongly with the anti-nuggets than H and He due to a Boltzmann enhancement.

Here we consider the effect of generic anti-macros on BBN. Anti-macros can affect BBN in several different ways. (See, e.g., Ref. [38] for a detailed discussion). They can annihilate with free protons and neutrons prior to BBN ($T > 10^{10}$ K), and they can annihilate with bound nucleons inside nuclei after BBN ($T < 10^9$ K). Photons or other particles from the annihilation process can themselves interact with (and fission) nuclei, and the light nuclei resulting from these fission and annihilation processes can yield alternative nucleosynthetic pathways. Here we will attempt only a rough order-of-magnitude estimate of these constraints. (See, e.g., Ref. [38] for a more detailed discussion).

We will derive the limit that can be placed on anti-macros from the annihilation of the anti-macro with a proton bound in a ^{4}He nucleus,

$$X + {}^4\mathrm{He} \rightarrow X' + {}^3\mathrm{He} + \gamma \,, \tag{8}$$

(where X' is the anti-macro X with its baryon number increased by 1), along with the requirement that ^{3}He not be overproduced by this process. We will not consider the additional photofission of ^{4}He from annihilation-produced photons because the emission spectrum around this epoch will peak in the several hundred keV range, which is far below the scales of $\sim$ 10 MeV needed to fission ^{4}He. The tail of the distribution may be important and this will be the subject of a follow up study. As such, we also do not consider the production of ^{6}Li from this ^{3}He; both of these processes are discussed in detail in Ref. [38]. Because the ^{4}He abundance produced by BBN is $\sim 10^5$ times the BBN ^{3}He abundance, even a tiny fraction of destroyed ^{4}He can be ruled out.

The number density of ^{3}He nuclei, relative to hydrogen, produced by the process in Eq. (8) at time t is given approximately by

$$({}^3\mathrm{He/H}) = ({}^4\mathrm{He/H})\, n_x \langle \sigma_x v \rangle t. \tag{9}$$

Because the macros are much more massive (and therefore moving more slowly) than the helium-4 nuclei, we can set $v \sim \sqrt{kT/m_{4He}}$. We also have ^{4}(He/H) $\approx 1/12$ and $n_x = \rho_{DM}/M_x$, where we will assume in this case that the anti-macros make up all of the dark matter ($\Omega_x \approx 0.25$). Then we have $n_x \approx 1.0 \times 10^{-31}\,\mathrm{cm}^{-3}\, T^3/M_x\,\mathrm{g/K}^3$. The time t is related to the temperature T during the epoch shortly after BBN by the relation $t = 1.8 \times 10^{20}\,\mathrm{sec(K}/T)^2$. Combining all of these, we obtain

$$({}^3\mathrm{He/H}) = 6.8 \times 10^{-9}\, T^{3/2} \sigma_x/M_x\,\mathrm{g\,cm}^{-2}\,\mathrm{K}^{-3/2}. \tag{10}$$

Eq. (10) gives roughly the helium-3 production produced by anti-macro annihilation on helium-4 at the temperature T. To get the best constraint, we set T to be the temperature at which BBN terminates, $T \approx 8 \times 10^8$ K, giving

$$({}^3\mathrm{He/H}) = 1.5 \times 10^5 (\sigma_x/M_x)\,\mathrm{g\,cm}^{-2} \tag{11}$$

The primordial abundance of helium-3 is poorly understood; Ref. [36] uses the constraint $({}^3\mathrm{He/H}) < 3 \times 10^{-5}$, while [38] takes $({}^3\mathrm{He/H})$ to be less than the primordial deuterium abundance (D/H) $\approx 2.6 \times 10^{-5}$ [39]. Substituting the CMB bound into Eq. (11) gives $({}^3\mathrm{He/H}) < 3.0 \times 10^{-5}$, which suggests that the CMB and BBN give similar constraints. However, given the crudeness of the current calculation, the CMB limit is more trustworthy. It is possible that a more detailed calculation utilizing a numerical calculation of the primordial element abundances could yield a tighter limit than our CMB constraint, but we would not expect an order of magnitude difference. This will be checked in a future study.

4. Human detectors

For a range of regular macro masses and cross sections, collisions with the human population would have caused a detectable number of serious injuries and deaths with obvious and unusual features, while there have been no reports of such injuries and deaths in regions of the world in which the human population is well-monitored. The region of parameter space where macros would have produced a devastating injury similar to a gunshot wound on the carefully monitored population of the Western world was thus constrained [15]. We use this same null result to constrain the same range of anti-macro masses, which deposit significantly more energy in human tissue. However, the signature will be different than in the previous study: in addition to the hole bored through the tissue, it is expected to be accompanied by a case of extreme radiation poisoning. We concentrate on this latter effect.

At 1 keV energies, which is a conservative underestimate as the spectrum may be harder, the photons possess a scattering length in human tissue of roughly 10^3 cm [40]. Thus, $1 - \exp(-0.05) \approx 10^{-2}$ of the energy from the emission at the surface of the anti-macro is deposited in a cylinder of radius 50 cm. To determine the total energy deposited, we multiply dE/dx in Eq. (1) by the path length of the macro inside the human body, which we assume to be $\sim$ 10 cm. The energy deposited in this radius of length 10 cm is

$$\Delta E = 10 \alpha \kappa \rho \sigma_x c^2 \,, \tag{12}$$

where $\alpha = 0.05$ is the fraction of energy that remains in the human tissue through the 1 keV photons that interact within 50 cm of the anti-macro surface and deposit their energy in the human tissue and $\kappa = 0.4$ is the fraction of energy that thermalizes and is eventually deposited into the human tissue.

The threshold for death to occur within a short period of time from exposure to high amounts of radiation is [41]

$$\frac{dE}{dm} \gtrsim 1000 Grays\,. \tag{13}$$

Requiring $\Delta E \geq 1000\,\mathrm{J} = 10^{10}$ ergs, we can rule out $\sigma_x \gtrsim 10^{-11}\,\mathrm{cm}^2$.

To constrain M_x, we consider the number of encounters between an anti-macro and the total number of humans in our sample

$$N_{events} = f \frac{\rho_{DM}}{M_x} N A t v_x \tag{14}$$

where $f = \Omega_x/\Omega_{DM}$ is the maximum allowed abundance of anti-macros that can contribute to the dark matter energy density in the Universe, $\rho_{DM} = 5 \times 10^{-25}\,\mathrm{g\,cm}^{-3}$ [42] and we have considered a monochromatic distribution of anti-macros with $n_x = \rho_{DM}/M_x$, $N = 8 \times 10^8$ is the total number of humans in our sample $A \sim 1\,\mathrm{m}^2$ is the cross-sectional area of a human, $t = 10$ years is the exposure time of our detector and v_x is the (relative) speed between the anti-macro and a human. (For more details, see the corresponding discussion in Ref. [15].)

Since the impact of an anti-macro is a Poisson process, the probability $P(n)$ of n impacts over the exposure time t follows the Poisson distribution

$$P(n) = \frac{{N_{events}}^n}{n!} e^{-N_{events}}\,, \tag{15}$$

where N_{events} is the expected number of events per interval and was given in Equation (14). If no events are observed, then the value $N_{events} \geq 3$ may be ruled out at 95% confidence, i.e. by requiring that the probability of no detected signals be less than 5%. This allows us to constrain the abundance of anti-macros as a function of the mass M_x

$$f \leq \frac{M_x}{5 \times 10^4\,\mathrm{g}}\,. \tag{16}$$

5. Other constraints

For many physical processes, the limits that can be placed on anti-macros are identical to the corresponding limits on macros. We discuss those limits briefly here.

5.1. Microlensing

For very large masses ($M_x \geq 10^{23}$ g), a variety of microlensing searches have constrained heavy composite object candidates [21–25] to make up at most a sub-leading component of the dark matter, regardless the nature of their non-gravitational interactions.

5.2. Paleo-detectors

Macros that would have penetrated a few km into the Earth's crust would have left tracks in ancient muscovite mica. Searches for grand-unified theory magnetic monopoles [19,20] sought to detect lattice defects left in ancient mica through chemical etching techniques. These limits were used to place limits on regular macros, over a wide range of cross-sections, up to $M_x = 55$ g [11] (this idea of using paleo-detectors to detect dark matter is not new; see [43,44] for an approach to detect WIMPs with paleo-detectors). We expect the elastic scattering cross-section of such objects to be of the same order as the annihilation cross-section for anti-macros [45][2] and so the same results apply as in the case of regular macros.

We have also suggested that, for appropriate M_x and σ_x, the passage of a macro through granite would form long tracks of melted and re-solidified rock that would be distinguishable from the surrounding unmelted granite [14]. A search for such tracks in commercially available granite slabs is planned. Using the same reasoning that allowed us to use the null result from the etching of ancient muscovite mica, anti-macros of the same minimum cross-section would have left visible tracks in the granite and so we expect the same results of hold. Thus, the results from the search of slabs of mica will apply to anti-macros as well.

5.3. Thermonuclear runaway

As discussed in [26] (and references therein), for thermonuclear runaway to be ignited, there is a minimum sized region, λ_{trig} that must be raised above a threshold temperature $T_{crit} \sim 3 \times 10^9$ K, where λ_{trig} is strongly dependent on density. Constraints were placed on elastically scattering macros using the continued existence of white dwarfs [26]. However, it was later determined that these constraints were too stringent; more accurate bounds were placed [17] although these bounds are subject to additional uncertainties. It has not been confirmed through numerical simulations that the conditions identified in [17,26] are indeed sufficient to initiate thermonuclear runaway, i.e., there remains some uncertainty whether in fact heating a region of size at least λ_{trig} to $T \sim$ few $\times 10^9$ K necessarily causes type 1A supernovae in white dwarfs and superbursts in neutron stars. In the case of anti-macros, the energy deposition is not expected to be much higher than the case of macros. This is because the emission temperature of the anti-macro is expected to be high enough that most of the positrons in the non-degenerate regime will be ionized.[3] Thus, λ_{trig} is still determined primarily by the cross-section of the anti-macro similar to the case of regular macros [17]. Emission from denser regions near the core is highly suppressed (see Appendix 4 in [4]).

6. Discussion and conclusions

We have considered a phenomenological approach and constrained the abundance of anti-macros over the relevant mass range based on several terrestrial, astrophysical and cosmological probes. Atomic density anti-macros are entirely ruled out by a combination of the CMB and microlensing constraints. Nuclear density macros are ruled out below 5×10^4 g, and possibly at some higher range mass windows through thermonuclear runaway. However those results are subject to additional uncertainties as discussed in Section 4.

We also note that such anti-matter objects could in principle alter the reionization history, as discussed in [46]. However, the most stringent constraints come from the early Universe due to the large number density of both the anti-macros and the protons. For objects below the grey bound in Fig. 1, which are significantly denser than atomic density objects, the number of encounters of an anti-macro with hydrogen atoms was found to be low enough that it will not significantly alter the recombination history nor

[2] No data exists to the best of our knowledge for antiproton energies of less than ~ 100 MeV. However, we expect that the order 1 difference between the annihilation and elastic scattering cross-sections at 100 MeV to not increase by several orders of magnitude at energies of several hundred keV.

[3] The temperature is higher in this case due to the larger number density of the target medium; see appendix A in reference [10].

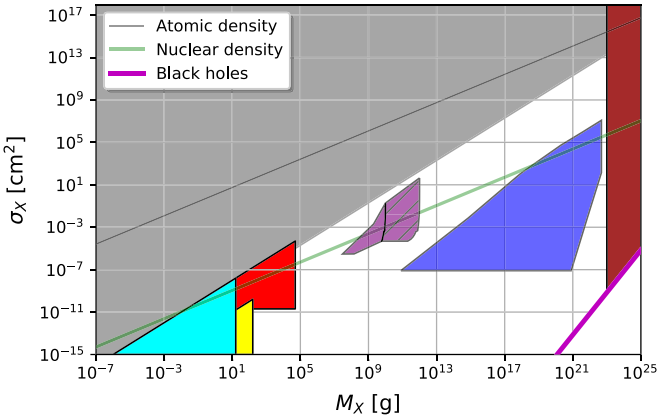

Fig. 1. Constraints on the anti-macro cross section and mass (assuming the anti-macros have a single mass). Constraints in brown come from various microlensing experiments, in yellow from a lack of tracks in an ancient slab of mica [19,20], in cyan from a lack of a signal in the Icecube experiment [10]; in grey from the Planck Cosmic Microwave Background, in red from a lack of human impacts, in light blue from thermonuclear runaway in white dwarfs and in light purple from a lack of superbursts over a period of a decade on the superburster 4U 1820-30. The hatched light purple region shows the region of parameter space that may be constrained from an analysis of all known local X-ray binaries and a better understanding of the mean background superburst rate [17]. The black and green lines correspond to objects of constant density $1\,\mathrm{g\,cm^{-3}}$ and $3.6\times10^{14}\,\mathrm{g\,cm^{-3}}$ respectively. Black hole candidates lie on the magenta line.

produce a higher extragalactic photon background around the 100 MeV range.

Declaration of competing interest

The authors declare that they have no known competing financial interests or personal relationships that could have appeared to influence the work reported in this paper.

Acknowledgements

This work was partially supported by Department of Energy grant de-sc0009946 to the particle astrophysics theory group at CWRU. R.J.S. was partially supported by the Department of Energy, de-sc0019207.

References

[1] M. Tanabashi, et al., Review of particle physics, Phys. Rev. D 98 (2018) 030001.
[2] E. Witten, Cosmic separation of phases, Phys. Rev. D 30 (1984) 272–285.
[3] Ariel R. Zhitnitsky, "Nonbaryonic" dark matter as baryonic color superconductor, J. Cosmol. Astropart. Phys. 2003 (2003) 010.
[4] Michael M. Forbes, Ariel R. Zhitnitsky, WMAP haze: directly observing dark matter?, Phys. Rev. D 78 (2008) 083505.
[5] Xunyu Liang, Ariel R. Zhitnitsky, Axion field and the quark nugget's formation at the QCD phase transition, Phys. Rev. D 94 (2016) 083502.
[6] Shuailiang Ge, Xunyu Liang, Ariel Zhitnitsky, Cosmological axion and quark nugget dark matter model, Phys. Rev. D 97 (2018) 043008.
[7] Nayyer Raza, Ludovic van Waerbeke, Ariel Zhitnitsky, Solar corona heating by the axion quark nugget dark matter, Phys. Rev. D 98 (2018) 103527.
[8] Victor V. Flambaum, Ariel R. Zhitnitsky, Primordial lithium puzzle and the axion quark nugget dark matter model, Phys. Rev. D 99 (2019) 023517.
[9] Shuailiang Ge, Kyle Lawson, Ariel Zhitnitsky, The axion quark nugget dark matter model: size distribution and survival pattern, Phys. Rev. D 99 (2019) 116017.
[10] Dmitry Budker, Victor V. Flambaum, Ariel Zhitnitsky, Axion quark nuggets. SkyQuakes and other mysterious explosions, arXiv:2003.07363, 2020.
[11] David M. Jacobs, Glenn D. Starkman, Bryan W. Lynn, Macro dark matter, Mon. Not. R. Astron. Soc. 450 (2015) 3418–3430.
[12] David M. Jacobs, Amanda Weltman, Glenn D. Starkman, Resonant bar detector constraints on macro dark matter, Phys. Rev. D 91 (2015) 115023.
[13] Jagjit SinghSidhu, Roshan MammenAbraham, Corbin Covault, Glenn Starkman, Macro detection using fluorescence detectors, J. Cosmol. Astropart. Phys. 1902 (2019) 037.
[14] Jagjit Singh Sidhu, Glenn Starkman, Ralph Harvey, A counter-top search for macroscopic dark matter, arXiv:1905.10025, 2019.
[15] Jagjit Singh Sidhu, Robert Scherrer, Glenn Starkman, Death and serious injury by dark matter, Phys. Lett. B 803 (2020) 135300.
[16] Jagjit Singh Sidhu, Glenn Starkman, Macroscopic dark matter constraints from bolide camera networks, Phys. Rev. D 100 (2019) 123008.
[17] Jagjit Singh Sidhu, Glenn Starkman, Reconsidering astrophysical constraints on macroscopic dark matter, Phys. Rev. D 101 (2020) 083503.
[18] Jagjit Singh Sidhu, Charge constraints of macroscopic dark matter, Phys. Rev. D 101 (2020) 043526.
[19] A. De Rujula, S.L. Glashow, Nuclearites: a novel form of cosmic radiation, Nature 312 (1984) 734–737.
[20] P.B. Price, Limits on contribution of cosmic nuclearites to galactic dark matter, Phys. Rev. D 38 (1988) 3813–3814.
[21] H. Niikura, et al., Microlensing constraints on primordial black holes with Subaru/HSC Andromeda observations, Nat. Astron. 3 (2019) 524–534.
[22] P. Tisserand, et al., Limits on the macho content of the galactic halo from the EROS-2 survey of the Magellanic clouds, Astron. Astrophys. 469 (2007) 387–404.
[23] C. Alcock, et al., MACHO project limits on black hole dark matter in the 1– 30 $M_\odot$ range, Astrophys. J. 550 (2001) L169–L172.
[24] B.J. Carr, Kazunori Kohri, Yuuiti Sendouda, Jun'ichi Yokoyama, New cosmological constraints on primordial black holes, Phys. Rev. D 81 (2010) 104019.
[25] Kim Griest, Agnieszka M. Cieplak, Matthew J. Lehner, New limits on primordial black hole dark matter from an analysis of Kepler source microlensing data, Phys. Rev. Lett. 111 (2013) 181302.
[26] Peter W. Graham, Ryan Janish, Vijay Narayan, Surjeet Rajendran, Paul Riggins, White dwarfs as dark matter detectors, Phys. Rev. D 11 (2018) 115027.
[27] Ryan J. Wilkinson, Julien Lesgourgues, Celine Boehm, Using the CMB angular power spectrum to study dark matter-photon interactions, J. Cosmol. Astropart. Phys. 2013 (2013) 026.
[28] Planck Collaboration, P.A.R. Ade, et al., Planck 2015 results. XIII. Cosmological parameters, Astron. Astrophys. 594 (2016) A13.
[29] Tracy R. Slatyer, Nikhil Padmanabhan, Douglas P. Finkbeiner, CMB constraints on WIMP annihilation: energy absorption during the recombination epoch, Phys. Rev. D 80 (2015) 043526.
[30] Claude Amsler, Nucleon-antinucleon annihilation at LEAR, arXiv:1908.08455, 2019.
[31] Claude Amsler, Proton-antiproton annihilation and meson spectroscopy with the Crystal Barrel, Rev. Mod. Phys. 70 (1998) 1293.
[32] V.M. Chechetkin, M.Yu. Khlopov, M.G. Sapozhnikov, Ya.B. Zeldovich, Astrophysical aspects of antiproton interaction with ^{4}He (antimatter in the universe), Phys. Lett. B 118 (1982) 329.
[33] David Lindley, Hadronic decays of cosmological gravitinos, Phys. Lett. B 171 (1986) 235.
[34] G. Yepes, R. Dominguez-Tenreiro, The effects of antimatter on primordial nucleosynthesis, Astrophys. J. 335 (1988) 3.
[35] Jan B. Rehm, Karsten Jedamzik, Big bang nucleosynthesis with matter-antimatter domains, Phys. Rev. Lett. 81 (1998) 3307.
[36] H. Kurki-Suonia, E. Sihvola, Constraining antimatter domains in the early universe with big bang nucleosynthesis, https://doi.org/10.1103/PhysRevLett.84.3756, 2000.
[37] H. Kurki-Suonio, E. Sihvola, Antimatter regions in the early universe and big bang nucleosynthesis, Phys. Rev. D 62 (2000) 103508.
[38] Jan B. Rehm, Karsten Jedamzik, Limits on matter-antimatter domains from big bang nucleosynthesis, Phys. Rev. D 63 (2001) 043509.
[39] Brian D. Fields, Keith A. Olive, Tsung-Han Yeh, Charles Young, Big-bang nucleosynthesis after Planck, J. Cosmol. Astropart. Phys. 3 (2020) 010.
[40] Stephen Seltzer, Tables of X-ray mass attenuation coefficients and mass energy-absorption coefficients, NIST Standard Reference Database 126, National Institute of Standards and Technology, https://doi.org/10.18434/T4D01F.
[41] Jerrold T. Bushberg, Radiation exposure and contamination - injuries; Poisoning, Merck Manuals Professional Edition, Last full review/revision Jul 2019, Accessed Jun 2020, https://www.merckmanuals.com/professional/injuries-poisoning/radiation-exposure-and-contamination/radiation-exposure-and-contamination.
[42] Jo Bovy, Scott Tremaine, On the local dark matter density, Astrophys. J. 756 (2012) 89.
[43] Thomas D.P. Edwards, Bradley J. Kavanagh, Christoph Weniger, Sebastian Baum, Andrzej K. Drukier, Katherine Freese, Maciej Górski, Patrick Stengel, Digging for dark matter: spectral analysis and discovery potential of paleo-detectors, Phys. Rev. D 99 (2019) 043541.
[44] Andrzej K. Drukier, Sebastian Baum, Katherine Freese, Maciej Górski, Patrick Stengel, Paleo-detectors: searching for dark matter with ancient minerals, Phys. Rev. D 99 (2019) 043014.
[45] Eberhard Klempt, Franco Bradamante, Anna Martin, Jean-Marc Richard, Antinucleon–nucleon interaction at low energy: scattering and protonium, Phys. Rep. 368 (2002) 119–316.
[46] S.I. Blinnikov, A.D. Dolgov, K.A. Postnov, Antimatter and antistars in the universe and in the Galaxy, Phys. Rev. D 92 (2015) 023516.